This procedure is effective, and normalization of coordinates possible, when the kinematic characteristics **h** and **i** can be presented as linear transformations of the respective configuration variables **h** and **l** (eq 30) and when the corresponding matrices (**C**, **D**) are symmetrical. In fact, the kinematics of entanglement networks is more complex; as evident from eq 23, the velocity of friction centers, **ṙ**, depends not only on the positions **r** but also on the sliding rates $\dot{L}_j$ and contour lengths L_j and cannot be reduced to linear relations assumed in eq 30. The same can be said about the other kinematic characteristic, **i̇**. Consequently, it cannot be shown what transformation would bring the problem to the "normal" form. It is not excluded though that some special cases of entanglement networks can still be described in terms of normal coordinates.

References and Notes

(1) P. E. Rouse, *J. Chem. Phys.*, **21**, 1272 (1953).
(2) B. H. Zimm, *J. Chem. Phys.*, **24**, 269 (1956).
(3) E. Guth and H. Mark, *Monatsh. Chem.*, **65**, 93 (1934).
(4) W. Kuhn, *Kolloid-Z.*, **68**, 2 (1934); *ibid.*, **76**, 258 (1936).
(5) P. J. Flory and J. Rehner, *J. Chem. Phys.*, **11**, 512 (1943).
(6) M. S. Green and A. V. Tobolsky, *J. Chem. Phys.*, **14**, 80 (1946).
(7) M. Yamamoto, *J. Phys. Soc. Jap.*, **11**, 413 (1956); *ibid.*, **12**, 1148 (1957); *ibid.*, **13**, 1200 (1958).
(8) A. S. Lodge, *Trans. Faraday Soc.*, **52**, 120 (1956).
(9) J. D. Ferry, R. F. Landel, and M. L. Williams, *J. Appl. Phys.*, **26**, 359 (1955); see also J. D. Ferry, "Viscoelasticity of Polymers," Wiley, New York, N. Y., 1970.
(10) F. Bueche, *J. Chem. Phys.*, **20**, 1959 (1952).
(11) M. Mooney, *J. Polym. Sci.*, **34**, 599 (1959).
(12) F. Bueche, *J. Chem. Phys.*, **25**, 599 (1956).
(13) F. Bueche, *J. Chem. Phys.*, **22**, 1570 (1954).
(14) W. W. Graessley, *J. Chem. Phys.*, **43**, 2696 (1963); *ibid.*, **47**, 1942 (1967).
(15) J. A. Duiser and A. J. Staverman in "Physics of Non-Crystalline Solids," North-Holland Publ. Co., Amsterdam, 1965; p 376; J. A. Duiser, Thesis, Leiden, 1965.
(16) A. J. Chömpff, Thesis, Delft, 1965; A. J. Chömpff and J. A. Duiser, *J. Chem. Phys.*, **45**, 1505 (1966).
(17) H. C. Booij and A. J. Staverman, IUPAC Symposium on Macromolecules, Leiden 1970, Preprints, p 255.
(18) M. Ilavský, J. Hasa, and I. Havlíček, *J. Polym. Sci., Part A-2*, **10**, 1775 (1972).
(19) W. C. Forsman and H. S. Grand, *Macromolecules*, **5**, 289 (1972).
(20) P. Thirion, Third Discussion Conference on "General Principles of Rheology," Prague, 1972, Paper B2.
(21) R. Takserman-Krozer and A. Ziabicki, *J. Polym. Sci., Part A-2*, **8**, 321 (1970).
(22) H. M. James and E. Guth, *J. Chem. Phys.*, **11**, 455 (1943); *ibid.*, **15**, 669 (1947).
(23) L. R. G. Treloar in "Physik der Hochpolymeren," H. A. Stuart, Ed., Vol. IV, Springer-Verlag, Berlin, 1956, p 295.
(24) A. Ziabicki, *Kolloid-Z. Z. Polym.*, in press.
(25) G. Marucci, G. Titomanlio, and G. C. Sarti, *Rheol. Acta*, **12**, 269 (1973).
(26) A. S. Lodge, *Rheol. Acta*, **7**, 379 (1968).

Conformational and Packing Stability of Crystalline Polymers. IV. Polyethers $[-O(CH_2)_m-]_n$ and Polythioethers $[-S(CH_2)_m-]_n$ with m = 2 and 3

Kazuo Tai and Hiroyuki Tadokoro*

Department of Polymer Science, Faculty of Science, Osaka University, Toyonaka, Osaka, 560 Japan.

Received October 29, 1973

ABSTRACT: Energy calculations covering both the helical and glide-type conformations have been derived, the planar zigzag being the special case of both these conformations. For the calculation, the intramolecular potential energy due to the internal rotation barriers, van der Waals interactions, and electrostatic interactions were taken into account. The stable conformations of polyethers $[-O(CH_2)_m-]_n$ with m = 2 and 3, *i.e.*, poly(ethylene oxide) (PEO) and polyoxacyclobutane (POCB), and polythioethers $[-S(CH_2)_m-]_n$ with m = 2 and 3, *i.e.*, poly(ethylene sulfide) (PES) and poly(trimethylene sulfide) (PTMS), were analyzed. According to the results of the calculations, the two modifications of PEO ((7/2) helix and planar zigzag), the conformation of PEO molecule in mercuric chloride complex type II, the three modifications of POCB (planar zigzag, glide type, and helix), and the conformations of the polythioethers, PES (glide type), and PTMS (G_4 type) were well explained. The intermolecular interaction energies in crystal for PEO, POCB, and PES were also calculated and discussed.

In a previous paper[1] of this series, the most stable conformations of several isotactic helical polymers were studied based upon the results of intramolecular energy calculations. The present study is an extention of this previous work and covers both helical and glide-type conformations, the planar zigzag being the special case of these conformations. The stable conformations of the polyethers $[-O(CH_2)_m-]_n$ with m = 2 and 3, *i.e.*, poly(ethylene oxide) (PEO) and polyoxacyclobutane (POCB), and polythioethers $[-S(CH_2)_m-]_n$ with m = 2 and 3, *i.e.*, poly(ethylene sulfide) (PES) and poly(trimethylene sulfide) (PTMS), were analyzed by this method and the results for polyethers were compared with those of corresponding polythioethers.

The conformational energy calculation under helical symmetry for PEO was reported by Magnasco *et al.*,[2] but such work as energy calculations covering both helical and glide-type conformations for these polyethers and polythioethers has not yet been reported.

Methods and Assumptions

Helical Conformations. In the case of the helical conformations, the energy calculations were made according to the same method described in the second paper[1] of this series; the fiber identity period was not fixed and it was only assumed that the chain forms a helical structure, *i.e.*, the set of the internal rotation angles repeats along the chain.

Glide-Type Conformation. For the glide-type conformations, the following two conditions are necessary:[3] (a) the signs of the corresponding internal rotation angles of the neighboring structural units are reversed, and (b) a translational unit consists of two structural units. The polymer chain having glide symmetry is shown as follows:

$$\begin{array}{ccccccccccccccccc} -M_{m'}{}^{n-1}- & M_1{}^n & -\cdots- & M_j{}^n & -\cdots- & M_m{}^n & -M_{1'}{}^n & -\cdots- & M_{j'}{}^n & -\cdots- & M_{m'}{}^n & -M_1{}^{n+1}- \\ & r_1 & & r_j & & r_m & r_1 & & r_j & & r_m & r_1 & \\ & \phi_1 & & \phi_j & & \phi_m & \phi_1 & & \phi_j & & \phi_m & \phi_1 & \\ & \tau_1 & & \tau_j & & \tau_m & \tau_{1'} & & \tau_{j'} & & \tau_{m'} & \tau_1 & \end{array}$$

where $M_j{}^n$ is the jth skeletal atom or group in the nth translational unit, r_j is the bond length between M_{j-1} and M_j, ϕ_j is the bond angle between the bond M_{j-1}—M_j and M_j—M_{j+1}, and τ_j is the internal rotation angle around the bond M_{j-1}—M_j (the prime indicates the succeeding monomer unit and the symbol n indicating the nth translational unit is omitted for simplicity, when it is not necessary.) The definition of the internal rotation angle is the same as that of reference 1.

The condition (a) is written as follows.

$$\begin{aligned} \tau_1 &= -\tau_{1'} \\ \tau_j &= -\tau_{j'} \\ \tau_m &= -\tau_{m'} \end{aligned} \tag{1}$$

Here we choose sets of right-handed cartesian coordinate systems in the following way (Figure 1). The origin of the coordinate system $\mathbf{x}_j$ coincides with the position of the M_j atom with its $\mathbf{x}_j$ axis on the bond M_j—M_{j+1}. The y_j axis lies on the plane determined by the two bonds M_j—M_{j+1} and M_{j-1}—M_j in such a way that the angle between the bond M_{j-1}—M_j and the positive direction of y_j is accute. According to the equation of Eyring, the transformation of the jth coordinates $\mathbf{x}_j$ into the $(j-1)$th $\mathbf{x}_{j-1}$ is expressed as

$$\mathbf{x}_{j-1} = \mathbf{A}_j\mathbf{x}_j + \mathbf{B}_j \tag{2}$$

where

$$\mathbf{A}_j = \begin{bmatrix} -\cos\phi_j & -\sin\phi_j & 0 \\ \cos\tau_j \sin\phi_j & -\cos\tau_j \cos\phi_j & -\sin\tau_j \\ \sin\tau_j \sin\phi_j & -\sin\tau_j \cos\phi_j & \cos\tau_j \end{bmatrix} \tag{3}$$

and

$$\mathbf{B}_j = \begin{bmatrix} r_j \\ 0 \\ 0 \end{bmatrix} \tag{4}$$

Then the transformation of the jth coordinates $\mathbf{x}_j{}^n$ of the nth translational unit into the jth coordinates $\mathbf{x}_j{}^{n-1}$ of the $(n-1)$th unit is expressed as

$$\mathbf{x}_j{}^{n-1} = \mathbf{A}\mathbf{x}_j{}^n + \mathbf{D}_j \tag{5}$$

where

$$\mathbf{A} = \mathbf{A}_{j+1}\cdots\mathbf{A}_m\mathbf{A}_{1'}\cdots\mathbf{A}_{m'}\mathbf{A}_1\cdots\mathbf{A}_j \tag{6}$$

and

$$\mathbf{D}_j = \mathbf{A}_{j+1}\cdots\mathbf{A}_{j-1}\mathbf{B}_j{}^n + \mathbf{A}_{j+1}\cdots\mathbf{A}_{j-2}\mathbf{B}_{j-1}{}^n + \cdots + \mathbf{A}_{j+1}\mathbf{B}_{j+2}{}^{n-1} + \mathbf{B}_{j+1}{}^{n-1} \tag{7}$$

$$\mathbf{B}_j{}^n = \mathbf{B}_j{}^{n-1} \tag{8}$$

$\mathbf{D}_j$ is the vector connecting $M_j{}^{n-1}$ and $M_j{}^n$ expressed by the $\mathbf{x}_j{}^{n-1}$ coordinate system.

We choose the other sets of right-handed cartesian coordinate systems $\xi_j{}^n(\xi_j, \eta_j, \zeta_j)$, as Shimanouchi and Mizushima[4] used in the case of helix (Figure 1). The origin of the coordinate system is on the foot of the perpendicular to the fiber axis drawn from $M_j{}^n$ atom, the $\xi_j{}^n$ axis being on this perpendicular with its positive direction pointing toward the $M_j{}^n$ atom. The $\zeta_j{}^n$ axis lies on the fiber axis. Then the transformation of the coordinates $\xi_j{}^n$ into $\xi_j{}^{n-1}$ can be expressed as

$$\xi_j{}^{n-1} = \mathbf{E}\xi_j{}^n + \mathbf{L} \tag{9}$$

where $\mathbf{E}$ is the unit matrix and $\mathbf{L}$ is the translation vector with its length being fiber identity period. The transformation of $\xi_j{}^n$ into $\mathbf{x}_j{}^n$ can be expressed as

$$\mathbf{x}_j{}^n = \mathbf{T}_j(\xi_j{}^n + \mathbf{S}_j) \tag{10}$$

where $\mathbf{T}_j$ is an orthogonal matrix and $\mathbf{S}_j$ is the vector connecting origins of both coordinate systems. From eq 5 and 10

$$\xi_j{}^{n-1} = \mathbf{T}_j{}^{-1}\mathbf{A}\mathbf{T}_j\xi_j{}^n + (\mathbf{T}_j{}^{-1}\mathbf{A}\mathbf{T}_j - \mathbf{E})\mathbf{S}_j + \mathbf{T}_j{}^{-1}\mathbf{D}_j \tag{11}$$

Since the eq 11 should be identical with eq 9, the following equations are obtained

$$\mathbf{T}_j{}^{-1}\mathbf{A}\mathbf{T}_j = \mathbf{E} \qquad \mathbf{A} = \mathbf{E} \tag{12}$$

$$\mathbf{L} = (\mathbf{T}_j{}^{-1}\mathbf{A}\mathbf{T}_j - \mathbf{E})\mathbf{S}_j + \mathbf{T}_j{}^{-1}\mathbf{D}_j = \mathbf{T}_j{}^{-1}\mathbf{D}_j \tag{13}$$

From eq 12

$$\text{Trace}\,(\mathbf{A}) = 3 \tag{14}$$

Equation 14 is equivalent to the aforementioned condition (b). In the actual calculation, the sets of the internal rotation angles which satisfy eq 1 and 14 were chosen.

Potential Functions and Molecular Parameters. The internal rotation barriers, van der Waals interactions, and electrostatic interactions were taken into account. The functions used are the sinusoidal type for the internal rotation barriers, Lennard-Jones 6-12 type for the van der Waals interactions, and the dipole-dipole interaction equation for the electrostatic interactions. The parameters of these energy functions are the same as those reported in reference 1 except for those associated with the sulfur atom. V_0(C—S) = 1.0 kcal/mol was estimated from the hindered rotation barriers of CH_3SH,[5] CH_3SCH_3,[6] and $CH_3SCH{=}CH_2$,[7] van der Waals radius of the S atom is 1.85 A,[8] the coefficient of the van der Waals attraction term for S···S was taken from the table of Eliel *et al.*,[9] the coefficients of those for S···H and S···C were estimated by the empirical combining law,[10] and the C—S bond moment was taken as 0.90 D.[11] The value of the dielectric constant was assumed to be 4.0 for all the materials treated here, because (1) this value has been used by many previous authors for various kinds of high polymers (polypeptides,[22-24] polyester,[25] and polysaccharides.[26]) and (2) the observed bulk dielectric constant of PEO is in the range of 4.0-4.5.[27] The numbering of the internal rotation angles is shown in Table I. The bond lengths and bond angles used are as follows: bond lengths, C—H = 1.10 Å, C—C = 1.54 Å, C—O = 1.43 Å, C—S = 1.815 Å; all bond angles = 109.5°.

Energy Calculations. Summation of the van der Waals and electrostatic interaction energies for both single polymer chains and crystals were made according to the eq 4-8 given in reference 12. The calculations covered all atom pairs and point-dipole pairs with distances shorter than 10 Å for the single polymer chains, and those shorter than 30 Å for the crystals. These cut-off distances were taken according to the results of the test calculations of

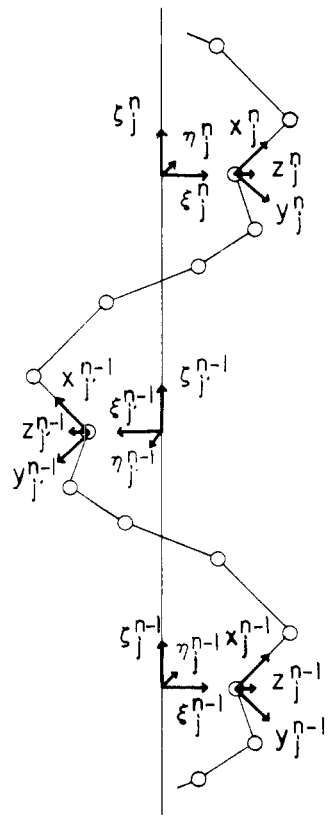

Figure 1. Schematic representation of the polymer chain having glide symmetry and the right-handed cartesian coordinates $\mathbf{x}_j^n(x_j, y_j, z_j)$ and $\xi_j^n(\xi_j, \eta_j, \zeta_j)$.

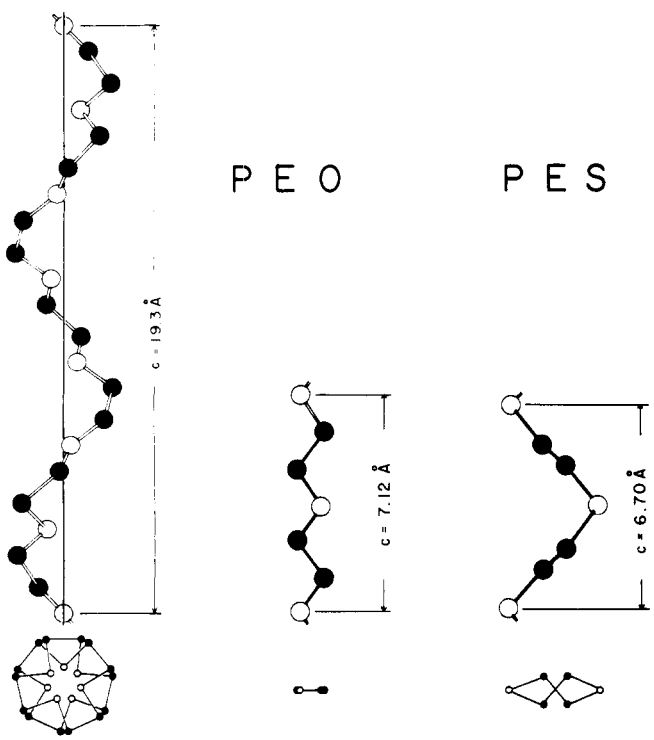

Figure 2. Molecular structures of the two modifications of PEO[13,15] and PES.[16]

dipole interaction (see Table II). The energy contour map obtained by the calculation for a single chain under helical symmetry has a high-energy band, where the helix pitch is zero and polymer chain forms a closed loop causing monomer unit to overlap, if a long enough chain is used for the calculations. The present calculations were

Table I
Definition of the Internal Rotation Angles and Molecular Conformations

τ_1	τ_2	τ_3	τ_4		
Poly(ethylene oxide) $-CH_2-[-O-CH_2-CH_2-]_n-$					
T	T	G		$(T_2G)_6$	Helix
T	T	T		(T_3)	Planar-zigzag
Poly(ethylene sulfide) $-CH_2-[-S-CH_2-CH_2-]_n-$					
G	G	T		$(\bar{G}_2T)$	Glide
Polyoxyacyclobutane $-CH_2-[-O-CH_2-CH_2-CH_2-]_n-$					
T	T	T	T		Planar zigzag
T	T	T	G	$(T_3\bar{G})$	Glide
T	T	G	G	(T_2G_2)	Helix
Poly(trimethylene sulfide) $-CH_2-[-S-CH_2-CH_2-CH_2-]_n-$					
G	G	G	G		Helix

Table II

	Cut-off Distance (Å)	Intermolecular Interactions[a]	Intramolecular Interactions[a]
PES	10	−0.085	0.136
	20	−0.101	0.138
	30	−0.102	0.138
POCB modification III	10	−0.017	−0.041
	20	−0.028	−0.040
	30	−0.028	−0.040

[a] kcal/mol of monomer unit.

made up to 20 monomer units for these 4 polymers in order to take into account this problem. For the calculations for glide symmetry, this problem does not appear and 6 monomer units were taken into account. The energy contours in the potential maps were drawn by interpolating the values at the points with 10° intervals of internal rotation angles. The more detailed calculations were made additionally with 5° intervals at the neighborhoods of potential minima when necessary. The intermolecular interaction energies of POCB, PEO, and PES were calculated for the crystal structures listed in Table III. These calculations were performed on a NEAC 2200 Model 700 digital computer in this university.

Results

Poly(ethylene oxide). PEO has two crystal modifications, the (7/2) helix[13,14] and planar-zigzag,[15] the molecular conformations of which are shown in Figure 2 and Table I. Although molecular conformation of the former one is considerably deformed from the uniform helix shown in Figure 2, according to the recent X-ray analysis,[14] we may regard it as a (7/2) uniform helix for the calculation of intramolecular interaction energy.

The energy map calculated for the helical conformation under dihedral symmetry ($\tau_1 = \tau_2$) is shown in Figure 3. The lower energy minima A ($\tau_1 = \tau_2 = 180°$, $\tau_3 = 60°$ and $-60°$, −1.9 kcal/mol of monomer unit) and B ($\tau_1 = \tau_2 = \tau_3 = 180°$, −2.0 kcal) closely correspond to the right- and left-handed (7/2) helices (•, actual structure of $\tau_1 = \tau_2 = \mp 171.75°$ and $\tau_3 = \pm 64.97°$[13]), and planar-zigzag conformation.[15] The broken lines in the figure are the high-energy bands due to the zero pitch helices.

The intermolecular interaction energies for both modifications were calculated according to their crystal structures[14,15] (Table III) and are shown in Table IV.

Table III
Crystallographic Data

Polymers	Molecular Conformations	Crystal System, Space Group, and Lattice Constants
Poly(ethylene oxide)	Helix[13,14]	Monoclinic, $P2_1/a - C_{2h}^5$, a = 8.16 Å, b = 12.99 Å, c = 19.30 Å, β = 126.1°
	Planar-zigzag[15]	Triclinic, $P\bar{1} - C_i^1$, a = 4.71 Å, b = 4.44 Å, c = 7.12 Å, α = 62.8°, β = 93.2°, γ = 111.4°
Poly(ethylene sulfide)	Glide[16]	Orthorhombic, $Pbcn - D_{2h}^{14}$, a = 8.50 Å, b = 4.95 Å, c = 6.70 Å
Polyoxacyclobutane	Glide[17]	Trigonal, $R3c - C_{3v}^6$, a = 14.13 Å, c = 8.41 Å
	Helix[17]	Orthorhombic, $C222_1 - D_2^5$, a = 9.23 Å, b = 4.82 Å, c = 7.21 Å

Table IV
Intra- and Intermolecular Potential Energy (kcal/mol of Monomer Unit)

	Intramolecular Contribution				Intermolecular Contribution			
Polymers	v.d.W.[a]	E.S.[b]	R.B.[c]	Total	v.d.W.	E.S.	Total	Total
PEO Helix	−1.8	0.15	0.1	−1.6	−6.2	−0.08	−6.3	−7.9
Zigzag	−1.9	0.01	0.0	−1.9	−6.0	−0.02	−6.0	−7.9
PES	−3.3	0.14	0.1	−3.1	−7.5	−0.10	−7.6	−10.7
POCB II	−3.4	−0.01	0.1	−3.3	−9.3	−0.03	−9.3	−12.6
III	−3.7	−0.04	0.0	−3.7	−9.2	−0.03	−9.3	−13.0

[a] Van der Waals nonbonded interaction energy. [b] Electrostatic interaction energy. [c] Rotation barrier.

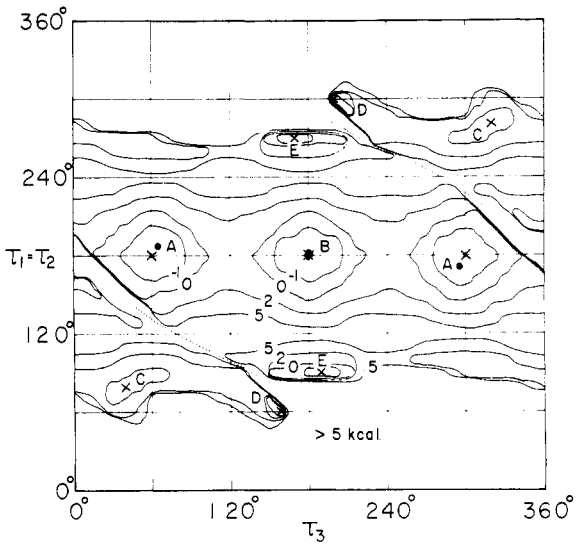

Figure 3. Potential energy map [$\tau_1(=\tau_2)$, τ_3] of PEO calculated for the helical conformation under dihedral symmetry. The energy minima are indicated by crosses, and the conformations determined by X-ray analyses are shown by closed circles.

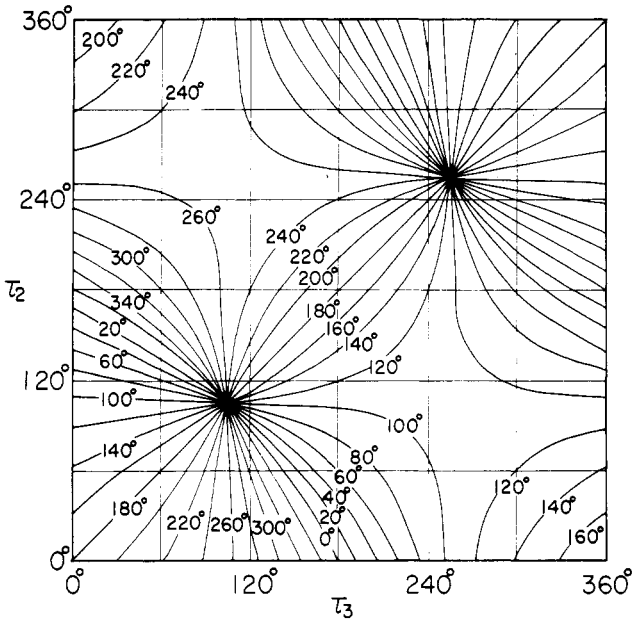

Figure 4. Three dimensional representation of the relation between τ_1, τ_2, and τ_3 of PEO, which satisfy the glide symmetry.

Next if we assume the glide symmetry with no other condition, the possible set of the internal rotation angles is on the curved surface in the cube defined by the three-dimensional cartesian coordinates, τ_1, τ_2, and τ_3, each covering from 0° to 360°. In Figure 4, the projection on the τ_2-τ_3 plane is shown and the corresponding τ_1 values are also given. The curved surface is symmetrical about the inversion center which is located on the point ($\tau_1 = \tau_2 = \tau_3 = 180°$) in the cube. The energy calculations were performed along the curves which are the intersections of the curved surface and the planes of $\tau_1 = 0°, 30°, \cdots, 180°$. It was found that the energy minima were obtained when τ_1 was in the range of 150–180°. Consequently, the more detailed calculations were made for τ_1 from 150 to 180°, τ_2 and τ_3 from 0 to 360° with intervals of 10°. In Figure 5 are shown the resultant potential energy curves. Two energy minima denoted by arrows were found at $\tau_1 = \tau_2 = \tau_3 = 180°$ (−2.0 kcal/mol of monomer unit), and $\tau_1 = 160°$, $\tau_2 = 70°$, and $\tau_3 = 50°$ (−1.4 kcal). The former corresponds to the planar-zigzag conformation, and the latter is similar to the conformation of PEO molecule in mercuric chloride complex type II.[18] The molecular structure of PEO in mercuric chloride complex is $\tau_1 = 167°$, $\tau_2 = 81°$, and $\tau_3 = 73°$. In this case, the intermolecular interactions with the mercuric chloride molecules were expected to be large. From the point of view that the PEO molecule is packed with mercuric chloride in the crystal lattice with the fiber identity period of 5.88 Å, the position on the curves of Figure 5 with this fiber identity period were marked by closed circles. The potential values indicated by the closed circles were plotted against τ_1 in Figure 6 and the energy minimum was found at $\tau_1 = 167°$, $\tau_2 = 80°$, and $\tau_3 = 73°$ (−0.6 kcal/mol of monomer unit). This conformation coincides closely with the actual conformation of PEO–$HgCl_2$ complex type II.

In order to compare with the glide-type conformation of PES, the energy calculations of PEO under glide symmetry were performed by assuming $\tau_1 = \tau_2$. Here the condi-

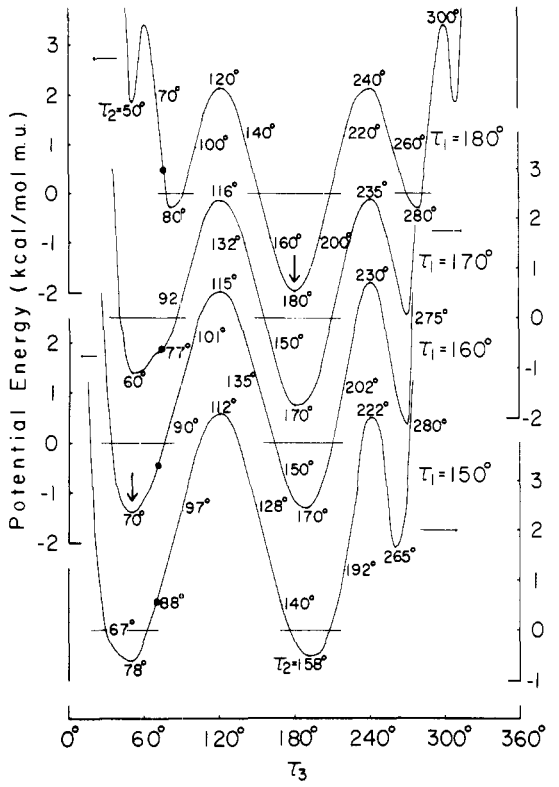

Figure 5. Potential energy plots of PEO along the curves which are the intersections of the curved surface and the planes of τ_1 = 150, 160, 170, and 180° (Figure 4), where τ_2 and τ_3 cover from 0 to 360° with the interval of 10°.

tion τ_3 = 180° or $\tau_1 = \tau_2 = \pm 104.5°$ becomes necessary as shown by Figure 4, and the number of the variables can be reduced from three to one. Since the latter condition gives models with high-energy value, only the result of the energy calculation under former condition is shown in Figure 7. The lowest minimum corresponds to the planar-zigzag conformation in contrast to the result for PES described later.

Polyoxacyclobutane. POCB has three crystal modifications, the molecular and crystal structures of which were determined by X-ray diffraction and infrared spectroscopic methods.[17,19] The molecular chain takes the conformations shown in Table I and Figure 8. Modifications I, II, and III are the planar-zigzag T_4, glide-type $T_3GT_3\bar{G}$, and helix $(T_2G_2)_2$, respectively. The potential energy calculations were made under the symmetry of glide and helix.

First we deal with the glide conformation. Although POCB has four kinds of internal rotation angles, three of the four become independent under glide symmetry. Then τ_1, τ_2, and τ_3 can take any point in the cube defined by the three-dimensional cartesian coordinates (τ_1, τ_2, τ_3), each covering from 0 to 360°, τ_4 being determined by the values of the other three variables. Energy calculations were performed by changing each torsional angle in the range of 0–330° with the intervals of 30° and the results are shown in Figure 9. Here, the τ_2–τ_3 sections of the energy contour are shown for τ_1 = 180°, 150°, ..., 60°. In the maps, the lowest energy values were taken, when the τ_4 values of more than one are found for a point in the cube. For example, in the case of τ_1 = 180°, the possible set of the internal rotation angles τ_2, τ_3, and τ_4 is on the two hatched planes in the τ_2, τ_3, τ_4 cube shown in Figure 10. In the cases of the τ_1 values other than 180°, the possible set is on the complicated curved surfaces. The results for the τ_1 values lower than 60° gave high-energy values

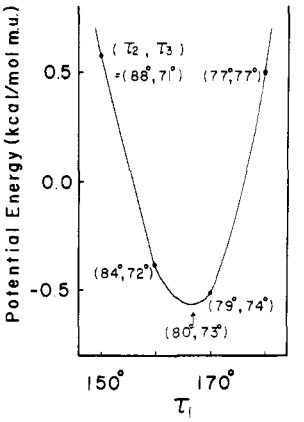

Figure 6. Potential energy curve obtained by tracing the closed circles (•) in Figure 5, where the conditions of the glide symmetry and the fiber identity period (= 5.88 Å) of PEO-$HgCl_2$ complex type II[18] were taken into account.

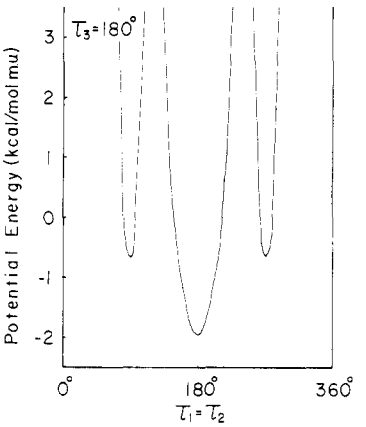

Figure 7. Potential energy curve of PEO plotted against $\tau_1 (= \tau_2)$ for τ_3 = 180°, where the conditions of the glide symmetry and the twofold rotation axes perpendicular to the fiber axis ($\tau_1 = \tau_2$) were taken into account.

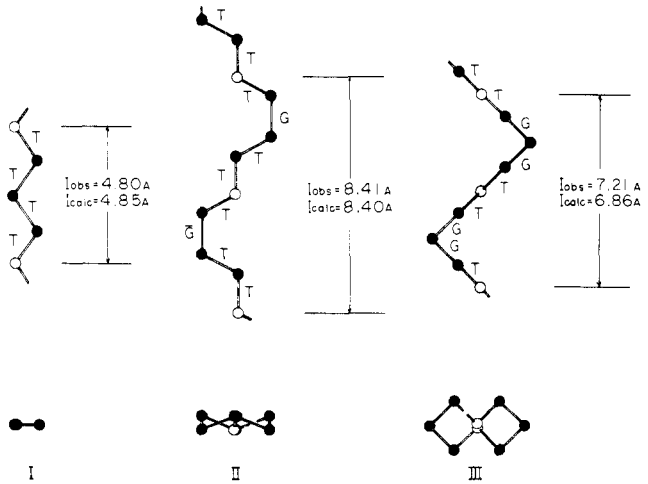

Figure 8. Molecular conformations of the three modifications of POCB.[17,19]

and are omitted from Figure 9 for simplicity. In Figure 9, the minima with the values lower than −2.3 kcal/mol of monomer unit were found only on the line $\tau_1 = \tau_2$ = 180°. This result indicates that the molecular chain consisted of the sequence —O—CH_2—CH_2—CH_2— is stable when the internal rotation angles around the C—O bonds are *T* (180°).

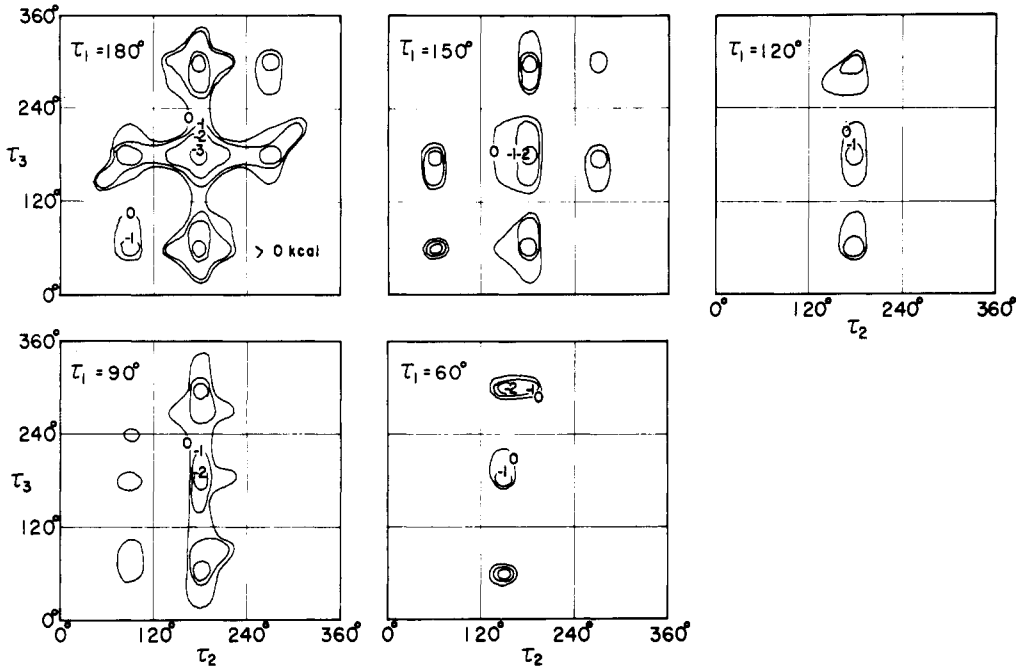

Figure 9. The τ_2–τ_3 sections of the potential energy contour of POCB under glide symmetry, for $\tau_1 = 180°, 150°, \cdots, 60°$.

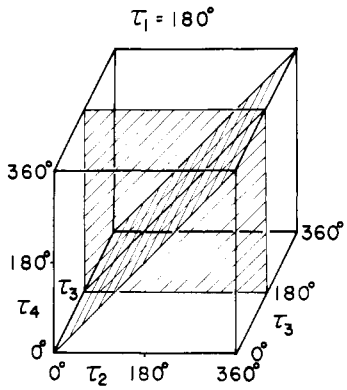

Figure 10. Schematic representation of the possible set of the internal rotation angles of τ_2, τ_3, and τ_4 of POCB under glide symmetry, when $\tau_1 = 180°$.

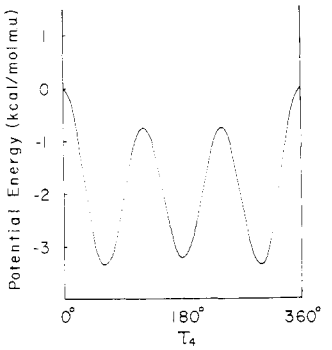

Figure 11. Potential energy curve of POCB plotted against τ_4 for $\tau_3 = 180°$, where the conditions of the glide symmetry and $\tau_1 = \tau_2 = 180°$ were taken into consideration.

Hence it may be reasonable to fix $\tau_1 = \tau_2 = 180°$, and this leads to a further condition $\tau_3 = 180°$ or $\tau_4 = 180°$. Here the potential energy plot for τ_4 was obtained under these conditions with the intervals of 10°, and is shown in Figure 11. This result gives three minima at $\tau_4 = 60°$ (−3.4 kcal/mol of monomer unit), −60° (−3.4 kcal), and 180° (−3.2 kcal), the former two corresponding to the $T_3GT_3\bar{G}$ glide type (modification II) and the latter to the planar-zigzag conformation.

For the helical conformation, two kinds of energy calculations were made. At first, the internal rotation angles τ_1 and τ_2 were fixed to 180°. The resultant τ_3–τ_4 energy map is shown in Figure 12. This map is symmetrical about the two diagonal lines. Three kinds of minima indicated by A (−3.6 kcal/mol of monomer unit), B (−3.2 kcal), and C (−3.4 kcal) were obtained. The minimum B corresponds to the T_4-type planar-zigzag conformation (modification I), and the minima A to the right- and left-handed $(T_2G_2)_2$-type helices (modification III). The T_3G-type helices corresponding to the minima C have not yet been found. There is a high-energy band along the diagonal connecting the two edges ($\tau_3 = 0°$, $\tau_4 = 360°$) and ($\tau_3 = 360°$, $\tau_4 = 0°$), except the special point ($\tau_3 = 180°$, $\tau_4 = 180°$) denoted by minimum B.

In the next calculation, we assumed the dihedral symmetry, *i.e.*, $\tau_1 = \tau_2$ and $\tau_3 = \tau_4$. In Figure 13 is shown the resultant energy contour map plotted against τ_1 (= τ_2) and τ_3 (= τ_4). There are four kinds of energy minima indicated by A (−3.6 kcal/mol of monomer unit), B (−3.2 kcal), C (−2.2 kcal), and D (−2.0 kcal). The map has inversion center at ($\tau_1 = \tau_2 = \tau_3 = \tau_4 = 180°$) and each kind of right-handed helix has a corresponding left-handed helical counterpart of the same energy. The high-energy band along a curve close to the diagonal connecting two edges ($\tau_1 = 0°$, $\tau_3 = 360°$) and ($\tau_1 = 360°$, $\tau_3 = 0°$) is also found. The minima A correspond to the $(T_2G_2)_2$-type helix of modification III and B to the planar-zigzag conformation of modification I. The conformations corresponding to the minor minima C and D have not yet been found.

The intermolecular interaction energies for the modifications II and III were calculated according to their crystal structures (Table III)[17] and the results are given in Table IV. Modification I will be treated elsewhere since this modification is a hydrate crystal and has a complicated problem concerning hydrogen bonding.

Poly(ethylene sulfide). The crystal structure of PES was determined by X-ray analysis[16] and the molecular chain takes a G_2TG_2T glide-type conformation shown in

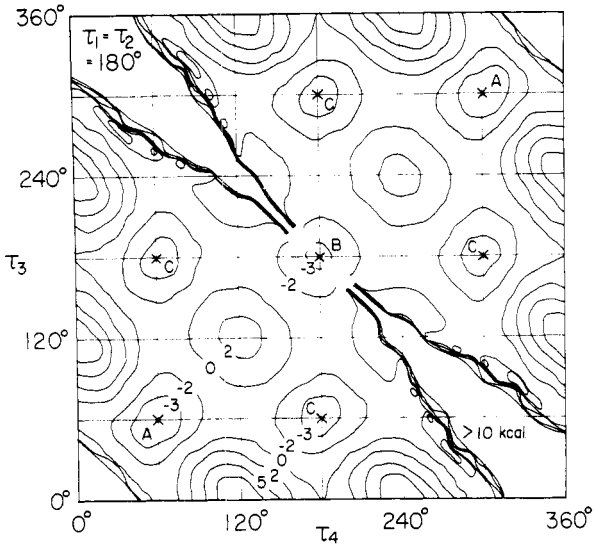

Figure 12. Potential energy map (τ_3, τ_4) of POCB calculated under the assumptions of the helical symmetry and $\tau_1 = \tau_2 = 180°$.

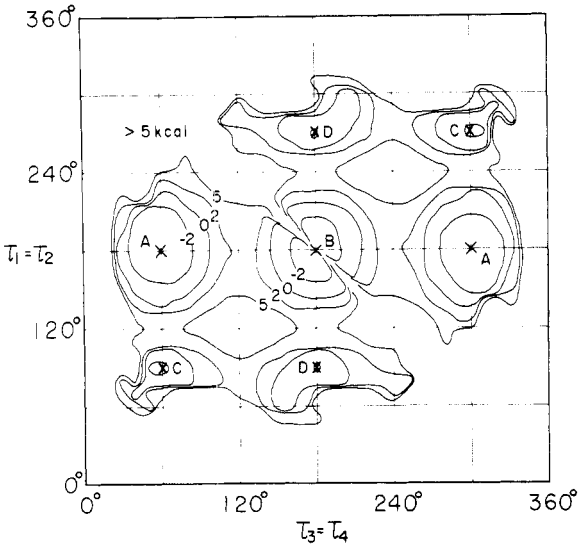

Figure 13. Potential energy map [$\tau_1(= \tau_2)$, $\tau_3(= \tau_4)$] of POCB calculated by assuming the helical symmetry and twofold rotation axes perpendicular to the helical axis.

Figure 2 and Table I. The energy calculations were performed under the helical and glide symmetry, assuming $\tau_1 = \tau_2$. The results of the calculations are shown in Figure 14 (helical conformation) and Figure 15 (glide-type conformation). These results correspond to those of PEO (Figures 3 and 7). All the energy minima in Figure 14 (helical conformation) have not yet been found. In this figure are found the high energy bands indicated by broken lines, just as the case of Figure 3 for PEO. In Figure 15, the lowest energy minima with −3.3 kcal/mol of monomer unit indicated by arrows correspond to the actual $G_2T\bar{G}_2T$ glide-type conformation. These results will be discussed in comparison with those of PEO in the following sections.

Intermolecular interaction energy was calculated according to the crystal structure (Table III)[16] and the result is given in Table IV.

Poly(trimethylene sulfide). According to the result of the X-ray analysis,[20] the conformation of PTMS is the G_4 type which has approximately twofold rotation axes passing through the sulfur atoms perpendicular to the fiber axis. Potential energy was calculated for helical conforma-

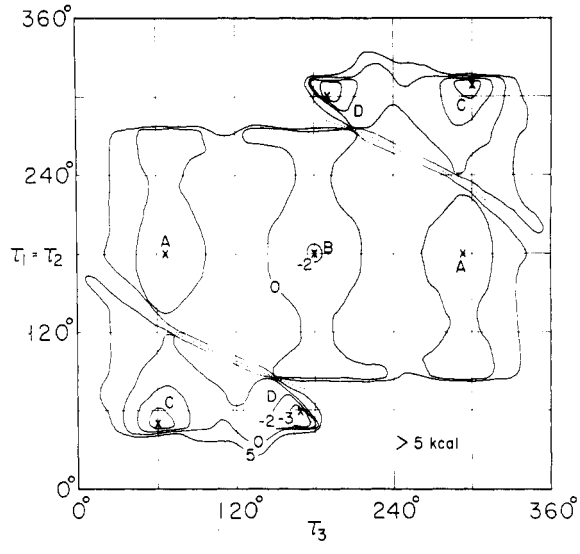

Figure 14. Potential energy map [$\tau_1(= \tau_2)$, τ_3] of PES calculated for helical conformation under dihedral symmetry.

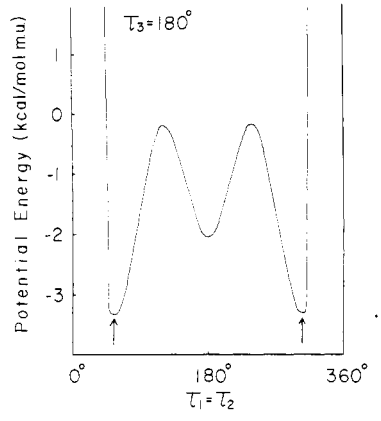

Figure 15. Potential energy curve of PES plotted against $\tau_1(= \tau_2)$ for $\tau_3 = 180°$, where the conditions of the glide symmetry and the twofold rotation axes ($\tau_1 = \tau_2$) were taken into account.

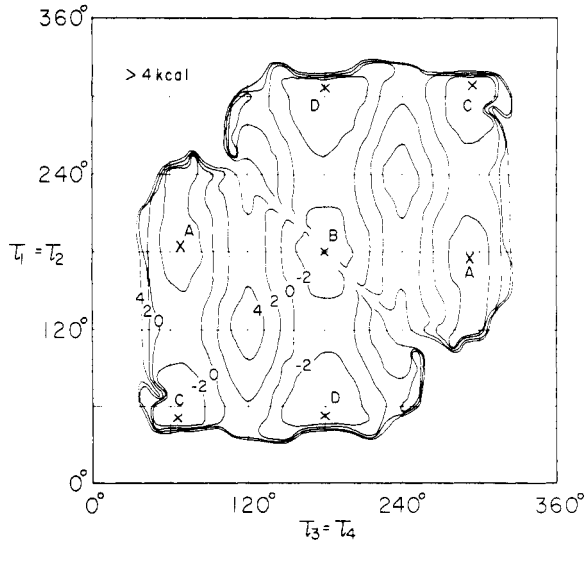

Figure 16. Potential energy map [$\tau_1(= \tau_2)$, $\tau_3(= \tau_4)$] of PTMS calculated by assuming the helical symmetry and the twofold rotation axes perpendicular to the helical axis.

tion by assuming the twofold rotation axes, *i.e.*, $\tau_1 = \tau_2$ and $\tau_3 = \tau_4$. Figure 16 is the energy contour map plotted against τ_1 (= τ_2) and τ_3 (= τ_4). There is an inversion center at the point ($\tau_1 = \tau_2 = 180°$, $\tau_3 = \tau_4 = 180°$) in this figure, just as the case of POCB (Figure 13). The positions of the potential energy minima are shown by the symbols A (−3.0 kcal/mol of monomer unit), B (−3.4 kcal), C (−4.6 kcal), and D (−4.9 kcal). The lowest energy minima D correspond to the $(G_2T_2)_2$-type helix, but this conformation has not yet been observed. The next lowest energy minima C correspond essentially to the G_4-type conformation of the actual existence. The minima A and B correspond to the hypothetical $(T_2G_2)_2$ helix and planar-zigzag conformations, respectively.

Discussion

Poly(ethylene oxide) and Poly(ethylene sulfide). As shown in Figure 2 and Table I, the molecular conformations of PEO and PES are quite different, although both polymers have similar chemical structures except for the oxygen and sulfur atoms. The conformation of PEO is just opposite to that of PES. In the case of PEO, the C—C bond takes the gauche form and the C—O bond the trans, while in the case of PES the C—C bond takes the trans and the C—S bond the gauche. It is interesting to elucidate the reason why such a difference exists in the molecular conformations of PEO and PES. The T_2G helical conformation of PEO and the G_2T glide-type conformation of PES could be well explained by the energy minima in Figures 3 and 15, respectively. Figures 7 and 15 give the results obtained by the same kind of energy calculations under the glide symmetry. The lowest energy minimum in Figure 15 (PES) corresponds to G_2T glide-type conformation, while the lowest minimum in Figure 7 (PEO) to the planar-zigzag conformation. The reason for the different conformations may be mainly attributable to the difference of the bond lengths of C—O (1.43 Å) and C—S (1.815 Å), and the van der Waals radii of the O (1.52 Å) and S (1.85 Å) atoms. When the internal rotation angle around the central C—O or C—S bond of the sequence of —CH_2*—CH_2—O(S)—CH_2*— is gauche, the nonbonded H···H distance (the H atoms indicated by asterisks) is 1.7 Å for PEO and 2.3 Å for PES. Accordingly the gauche conformation is prevented by the steric hindrance for the C—O bond of PEO, but is much favorable for the C—S bond of PES, since the van der Waals radius of the H atom is 1.1–1.2 Å. Although the lowest energy minima D on the map for PES calculated under helical symmetry (Figure 14) correspond to the right- and left-handed helices of G_2T type, this type of conformation has not yet been found. From this result, it can be clearly understood that the G_2T-type local conformation of PES is stable and if we set the internal rotation angles of the subsequent monomer unit to be inversed (from G to $\bar{G}$), the G_2T-type helix is transformed into the $G_2T\bar{G}_2T$ glide-type conformation. The reason why the G_2T-type helix has not yet been found is not obvious, but the possibility of poor packing in the lattice may be a case. In the actual crystal structure, the molecular chains are well packed, the intermolecular interaction energy being −7.6 kcal/mol of monomer unit as shown in Table IV. The other minor minima C, D, and E of PEO (Figure 3) and A, B, and C of PES (Figure 14) were also found, but the conformations corresponding to these minima have not been observed.

The conformational analysis for PEO under helical symmetry was performed by Magnasco *et al.*[2] In their potential energy map which corresponds to the Figure 3 of this study, there are two kinds of energy minima explaining the T_2G-type helix and planar-zigzag, but the high-energy band due to the zero pitch helices which should be in the map cannot be found. In a previous paper,[21] the authors reported the energy calculations made under the assumptions of the (7/2) helical symmetry and the fixed fiber identity period. This condition is equivalent to fixing the helical pitch and the helical turn of the monomer unit. The result explained well the T_2G helix as a lowest energy minimum, while the other minor minima having the internal rotation angle 75° around the C—O bond are also found.

Poly(ethylene oxide)-Mercuric Chloride Complex Type II. On the process of the energy calculations described above, we could find some minor minima which do not correspond to the actual structure. For example, in Figure 5 showing the results of the energy calculations under glide symmetry for PEO, there are two minima indicated by arrows. The lowest energy minimum with −2.0 kcal/mol of monomer unit ($\tau_1 = \tau_2 = \tau_3 = 180°$) corresponds to the planar-zigzag of actual existence and the minor one with −1.4 kcal/mol ($\tau_1 = 160°$, $\tau_2 = 70°$, $\tau_3 = 50°$) to the $TG_2T\bar{G}_2$ glide-type conformation not found as a modification of PEO crystal. However, this $TG_2T\bar{G}_2$ glide-type conformation is considered to be stabilized in the crystal lattice of mercuric chloride complex type II by large intermolecular interaction energy. Therefore the conformations of energy minima which do not correspond to the actual structure of the polymer itself can also become stable, if large enough stabilizing energy such as complex formation is affected to the molecular chain in the crystal lattice.

Polyoxacyclobutane and Poly(trimethylene sulfide). For POCB, the potential energy minima denoted by C in the energy map calculated under the helical symmetry (Figure 12) correspond to the right- and left-handed T_3G-type (3/1) helices. These helical conformations are absent in the crystal modifications of POCB, and the actual structure found out as modification II is the $T_3GT_3\bar{G}$ glide-type conformation having the same local conformation of monomer unit. In this case, the suitable packing of the molecular chain in the crystal lattice could stabilize $T_3GT_3\bar{G}$ glide-type conformation, as we discussed in the case of G_2T-type conformation of PES.

In Figures 13 and 16 are shown the results of the energy calculations under helical symmetry for POCB and PTMS, assuming the dihedral symmetry. The potential energy minima A, B, C, and D for POCB shown in Figure 13 correspond to those of PTMS in Figure 16, though the precise position of the minima are appreciably different from each other except B. Among these minima, lower minima A and B of POCB and C of PTMS are actually found. It may be pointed out that the energy differences between the conformations which actually exist and do not are about 1.0 kcal/mol of monomer unit for both polymers except the minima D of PTMS.

Stability of the Modifications. The calculations of the potential energies for the crystals gave the total energy values roughly the same for the two modifications of PEO, although the helix modification is experimentally far more stable than the planar zigzag. For POCB, the calculated result shows that modification III is more stable than modification II by 0.4 kcal/mol of monomer unit. However this energy difference has no significant meaning, because of the following reasons. (a) The semiempirical potential functions assumed here are not adequate for the discussion about such a slight energy difference. It may be possible that slight perturbation of the crystal structure produces larger variations of energy value. (b) The stability must be compared by the free energy. For an ideal crystal, the entropy term of the free energy is due to the vibra-

tional contribution, and the evaluation of the vibrational free energy requires a complete normal mode analysis of the crystal lattice. In addition, for actual crystals, the entropy term due to the crystal defect and incoherent molecular motion at high temperature may play an important role in the stabilization of the crystal.

In this paper, however, only the static potential energy term which would occupy the largest part of the free energy was discussed as a first approximation.

Acknowledgment. The authors express their sincere thanks to Dr. M. Kobayashi of this laboratory for his helpful advice and fruitful discussion.

References and Notes

(1) H. Tadokoro, K. Tai, M. Yokoyama, and M. Kobayashi, *J. Polym. Sci. Polym. Phys. Ed.*, 11, 825 (1973).
(2) V. Magnasco, G. Gay, and C. Nicora, *Nuovo Cimento*, 34, 1263 (1964).
(3) P. Ganis and P. A. Temussi, *Makromol. Chem.*, 89, 1 (1965).
(4) T. Shimanouchi and S. Mizushima, *J. Chem. Phys.*, 23, 707 (1955).
(5) R. W. Kilb, *J. Chem. Phys.*, 23, 1736 (1955).
(6) L. Pierce and M. Hayashi, *J. Chem. Phys.*, 35, 479 (1961).
(7) R. E. Penn and R. F. Curl, Jr., *J. Mol. Spectrosc.*, 24, 235 (1967).
(8) L. Pauling, "The Nature of the Chemical Bond," 3rd ed., Cornell University Press, Ithaca, N. Y., 1960.
(9) E. L. Eliel, A. L. Allinger, S. J. Angyal, and G. A. Morrison, "Conformational Analysis," Wiley, New York, N. Y., 1965.
(10) G. H. Hudson and J. C. McCoubrey, *Trans. Faraday Soc.*, 56, 761 (1960).
(11) G. P. Smyth, "Dielectric Behavior and Structure," McGraw-Hill, New York, N. Y., 1955, p 244.
(12) R. Hasegawa, M. Kobayashi, and H. Tadokoro, *Polym. J.*, 3, 591 (1972).
(13) H. Tadokoro, Y. Chatani, T. Yoshihara, S. Tahara, and S. Murahashi, *Makromol. Chem.*, 73, 109 (1964).
(14) Y. Takahashi and H. Tadokoro, *Macromolecules*, 6, 672 (1973).
(15) Y. Takahashi, I. Sumita, and H. Tadokoro, *J. Polym. Sci. Polym. Phys. Ed.*, 11, 2113 (1973).
(16) Y. Takashashi, H. Tadokoro, and Y. Chatani, *J. Macromol. Sci. Phys., B*, 2, 361 (1968).
(17) H. Tadokoro, Y. Takahashi, Y. Chatani, and H. Kakida, *Makromol. Chem.*, 109, 96 (1967).
(18) M. Yokoyama, T. Ishihara, R. Iwamoto, and H. Tadokoro, *Macromolecules*, 2, 184 (1969).
(19) H. Kakida, D. Makino, Y. Chatani, M. Kobayashi, and H. Tadokoro, *Macromolecules*, 3, 569 (1970).
(20) H. Sakakihara-Kitahama, Y. Takahashi, and H. Tadokoro, unpublished data.
(21) H. Sakakihara-Kitahama and H. Tadokoro, *J. Macromol. Sci. Phys., B*, in press.
(22) D. A. Brant and P. J. Flory, *J. Amer. Chem. Soc.*, 87, 2791 (1965).
(23) R. A. Scott and H. A. Scheraga, *J. Chem. Phys.*, 45, 2901 (1966).
(24) T. Ooi, R. A. Scott, G. Vanderkooi, and H. A. Scheraga, *J. Chem. Phys.*, 46, 4410 (1967).
(25) D. A. Brant, A. E. Tonelli, and P. J. Flory, *Macromolecules*, 2, 228 (1969).
(26) C. V. Goebel, W. L. Dimpfl, and D. A. Brant, *Macromolecules*, 3, 644 (1970).
(27) N. G. McCrum, B. E. Read, and G. Williams, "Anelastic and Dielectric Effects in Polymeric Solids," Wiley, London, 1967.

Light-Scattering Studies of a Polystyrene–Poly(methyl methacrylate) Two-Block Copolymer in Mixed Solvents

Hiroyasu Utiyama, Kunihiro Takenaka, Motoo Mizumori, Mitsutoshi Fukuda, Yoshisuke Tsunashima, and Michio Kurata*

Institute for Chemical Research and Department of Industrial Chemistry, Kyoto University, Kyoto, Japan. *Received October 25, 1973*

ABSTRACT: Light-scattering measurements were made on a two-block copolymer of polystyrene and poly(methyl methacrylate) whose molecular weight and styrene content by weight are 1.53×10^6 and 0.38, respectively. Mixtures of toluene and furfuryl alcohol of various compositions were used as solvent. They are both good as solvent for poly(methyl methacrylate) and isorefractive as well, but the latter is a nonsolvent for polystyrene. The results show that the mean-square radius of the polystyrene subchain in the isolated block copolymer always exceeds the value for the homopolystyrene of equal molecular weight. This result confirms the view that intramolecular contacts of dissimilar units do occur. The intermolecular micelle formation set in at a solvent composition between 36.7 and 38.9 wt % of toluene. The largest micelle formed at 19.8% comprised about 72 molecules. From the shape of the particle scattering function we have concluded that the polystyrene subchain forms a core of anisotropic shape in the beginning of aggregation but cores in larger micelles assume the shape of dense sphere. Solutions of isolated molecules and micelles both revealed an anomalous upsweep of the reciprocal scattering function at small scattering angles but the anomaly became more pronounced for larger micelles as evidenced by a longer correlation distance. This result suggests for the micelle such a conformation as the dense polystyrene core thickly surrounded by extended chains of poly(methyl methacrylate).

In the previous light-scattering study on a two-block copolymer of polystyrene (PS) and poly(methyl methacrylate) (PMMA),[1] we compared the size of the PS subchain with that of the isolated PS of equal molecular weight in solvents that are good solvents for both PS and PMMA and isorefractive as well to PMMA.[2] In the present work we have investigated the conformation of the two-block copolymer in poor solvents for PS. Of special interest to us is the investigation of the extent to which the size of the PS subchain is diminished in increasingly poor solvents before molecules undergo the intermolecular aggregation. It is also important to elucidate the size and conformation of the micelle in relation to the process of the domain formation in films cast from block copolymer solutions.[3] Krause found almost a decade ago[4] that three-block copolymers of PMMA–PS–PMMA form stable aggregates which are in a state of thermodynamic equilibrium. It may be interesting to investigate further the process of micelle formation by adopting the approach initiated by Leng and Benoit[5] and adopted also in our previous study, *i.e.*, to utilize as solvent a liquid giving a very low value of refractive index increment for PMMA. The analysis of the experimental angular variation of light scattering at infinite dilution is then straightforward. We thus decided to choose as solvent a mixture of two liquids which meet the following specifications: (1) they are both